Anodizing process of Al films on Si substrates for forming alumina templates with short-distance ordered 25 nm nanopores

Y.F. Mei [a], X.L. Wu [a,*], T. Qiu [a], X.F. Shao [a], G.G. Siu [b], Paul K. Chu [b]

[a]National Laboratory of Solid State Microstructures and Department of Physics, Nanjing University, Nanjing 210093, PR China
[b]Department of Physics and Materials Science, City University of Hong Kong, Kowloon, Hong Kong, PR China

Abstract

Porous alumina templates with short-distance ordered 25 nm nanopores were fabricated by controlling anodizing progress of Al films on Si substrates in sulfuric acid solution. The ordering of nanopore arrangement with a hexagonal symmetry was found to be closely related to thickness of the deposited Al film, growth temperature, applied voltage, and solution concentration. These parameters were explored in detail and proper experimental conditions were obtained to be 0.44 μm, 5 °C, 20 V, and 15 wt.% for the formation of a relatively ordered nanopore array. Anodizing progress of the Al film was monitored through the current–time ($I-t$) curve. Infrared transmittance spectral characterization and microstructural observations disclose that a SiO_2 island array has been formed on the surface of Si substrate under our experimental conditions. This kind of SiO_2 island array can be expected to have applications in nanoelectronics and optoelectronics.
© 2005 Elsevier B.V. All rights reserved.

1. Introduction

Using the templates of anodic porous alumina (APA), many nanostructures, including semiconductors, metals, and metal oxide, have been obtained through chemical [1] or physical [2] methods such as metal Ni (Te, Cu, and Fe) nanowires [3–5], metal Pt (Au and Pd) nanoholes [6], semiconductor CdS (CdSe and CdTe) nanowires [7–9], and TiO_2 nanotubes [10,11]. Especially, carbon nanotubes, promising in nanoelectronic devices, have been fabricated with different diameters, lengths, and spatial arrangements via the APA templates [12–14]. In addition, Y-junction carbon nanotubes, which represent new heterojunctions for nanoelectronics, have also been synthesized using Y-branched nanochannel APA templates [15,16].

On the other hand, Si-based nanostructures have attracted considerable interest in recent years because of their applications in nanoelectronics [17] and optoelectronics [18]. Therefore, the APA templates formed on Si substrates are of more important significance in applications. As a template, the APA film formed on bulk Al could show highly self-ordered hexagonal nanopore array with different pore diameters [19,20], but for the APA film on Si substrate highly ordered nanopore array is difficult to be formed mainly due to the complicated surface states (roughness and crystallite sizes) and non-uniformity of the deposited Al film [21,22]. This will directly affect the ordering of the fabricated nanostructures. Thus, it is very necessary to investigate in detail the nanopore growth of the APA film on Si substrate. Since the APA film with 25 nm nanopores has special significance in fabricating the nanostructured materials with quantum confinement effect [2,23,24], in this work we draw our attention to the growth process of the APA template on Si substrate with 25 nm nanopores [25–27]. Various growth conditions were explored and proper

---

* Corresponding author.
    E-mail address: hkxlwu@nju.edu.cn (X.L. Wu).

experimental parameters were obtained for the formation of a relatively ordered nanopore array. By analyzing the current–time ($I-t$) curve of anodizing process and infrared transmittance spectra of the obtained samples, we identify the formation of a SiO_2 island array on Si substrate. This kind of SiO_2 island array can be expected to have applications in modern nanodevices.

2. Samples and experiments

The substrates used in this work were <100>-oriented p-type silicon wafers with a resistivity of 5 Ω cm. A layer of thin Al film with a purity of 99.99% was deposited onto the Si wafer using electron beam evaporation. The Al film thicknesses were selected to be 0.22, 0.44, and 1.0 μm, respectively. No pretreatments were performed prior to the anodization. Anodization with a platinum plate as a cathode and the Al/Si system as anode was carried out in a sulfuric acid under a constant dc voltage. By monitoring the $I-t$ curve, the anodization of the Al/Si system can easily be controlled and the APA film can be detached from the Si substrate [2]. In our experiments, several types of silicon substrates with different orientations have been used and no noticeable changes have been found for the $I-t$ curve.

Fourier-transform infrared (FTIR) transmittance spectra were taken on a Nicolet 170 SX spectrometer at a resolution of 2 cm^{-1}. To obtain the film signal, we measured the FTIR spectra of a standard Si substrate and the films with Si substrates. After subtracting the substrate signal, we obtain the FTIR data from the films themselves. Transmission electron microscope (TEM) observations were carried out on a Hitachi H-800-NA microscope operated at 200 keV. The TEM samples prepared for top view were directly from the APA films, which were detached from the Si substrates. We found that for the TEM sample near the bottom of porous alumina film, it usually exhibits more ordered pore-arrangement than that near the surface region. Thus, in order to obtain a comparable result, we used the TEM sample near the surface region. Atomic force microscopy (AFM) image (512 × 512) was obtained on a Nanoscope IIIa of Digital Instruments Veeco Metrology Group working in contact mode, using commercial Si_3N_4 cantilever (Type NP-S20) with a spring constant of 0.58 Nm^{-1}. The scan rate is 0.5549 Hz.

3. Results and discussions

Previously, we have known that the APA film on bulk Al can have a perfect hexagonal pore arrangement using two kinds of fabrication methods, one being long time anodization of Al wafer and the other the anodization of Al wafer with mold of small regular pores on the surface [28]. In our current samples, due to the thin thickness of the deposited Al film (<0.5 μm), the arrangement of nanopores in the

APA film was found to be far from ordering. To improve the ordering of nanopore arrangement, we made a series of experiments by changing various experimental parameters, mainly including the applied voltage, the solution concentration, the thickness of the deposited Al film, and the growth temperature. Under an applied voltage of ~20 V, we found that the ordering can be greatly improved. When the voltage is more than 30 V, a stable anodization is difficult to be maintained due to easy detachment and splitting of the Al film. When the applied voltage is less than 20 V, although anodic process is stable, the nanopore growth is rather irregular. This leads to a disordering of nanopore arrangement. Therefore, in the present experimental conditions we choose 20 V to grow the APA film on Si substrate. As for the influence of sulfuric acid concentration on the ordering of nanopore arrangement, we tested a series of sulfuric acid concentrations from 5 to 30 wt.% and found that the solution with a concentration of 15 wt.% is the most suitable for fabrication of the APA film with a relatively ordered nanopore array.

For Al foil, a long-time anodization can lead to the formation of a highly ordered nanopore array. This implies that the influence of the surface states can partially be overcome by using a thick Al film. Therefore, it is also important to investigate the influence of the thickness of the deposited Al film on the growth of ordered nanopores. Since we used the same experimental conditions for the deposition of various Al films, we can suppose that the surface states of the deposited Al films with different thicknesses are basically the same and the influence on the ordering of pore-arrangement mainly depends on the Al film thickness. In our current investigation, we used the Al films with thicknesses of 0.22, 0.44, and 1.0 μm to carry out anodization and found that the 1.0 μm Al film is easy to fall off during anodization. For the 0.22 and 0.44 μm Al films, the shapes and ordering of self-organized nanopores are very different, as shown in Figs. 1(a) and (b),
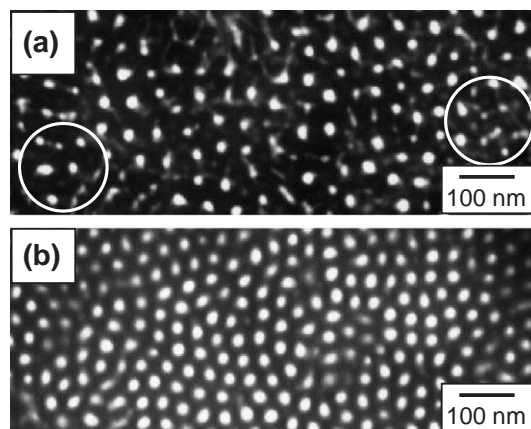

Fig. 1. Planar TEM images of the APA templates with 25 nm nanopores. The thicknesses of the deposition Al films are (a) 0.22 and (b) 0.44 μm. The anodizing process of the Al/Si system was conducted under a constant voltage of 20 V, a sulfuric acid concentration of 15 wt.%, and a growth temperature of 5 °C.
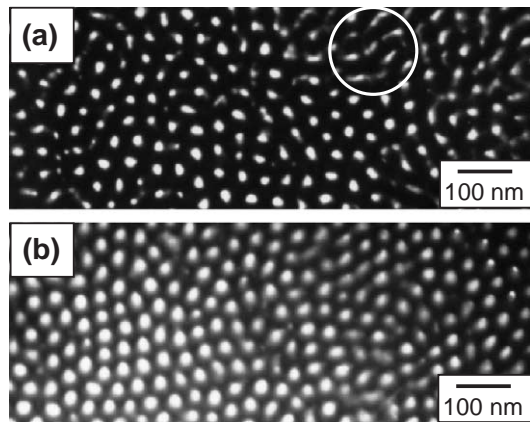
Fig. 2. Planar TEM images of the APA templates with 25 nm nanopores formed at different growth temperatures: (a) 27 and (b) 5 °C. The anodizing process of the Al/Si system was conducted under a constant voltage of 20 V, a sulfuric acid concentration of 15 wt.%, and an Al film thickness of 0.44 μm.

respectively. It can be seen that the 0.44 μm Al film has relatively uniform 25 nm nanopores after the anodization. Their arrangement is short-distance ordered and displays a hexagonal symmetry. The interpore distance is about 50 nm. However, for the 0.22 μm Al film, the nanopores show irregular shapes and the arrangement is also much less ordered (see the circles). Shown in Figs. 2(a) and (b) are two TEM images of the APA films grown in the solutions with different temperatures. One can find that the anodization in a solution of 5 °C could lead to more regular nanopore shapes and higher ordering of nanopore arrangement [Fig. 2(b)] than that in a solution of 27 °C (room temperature) [Fig. 2(a)], although the latter can lead to slightly smaller nanopore diameters (<25 nm) than the former. This difference can be explained as follows: During the anodization, joule heating occurs at the Al oxide/solution interface. Because the Al oxide is a thermal insulant, over-heating in local region will cause thermal agitation, which affects the uniform growth and ordered arrangement of nanopores. Meanwhile, heat dissipation will give rise to the fluctuation of anodizing current [29], which will also deduce irregular arrangement of nanopores. To give the influence of the anodizing current on the ordering of pore array, we used slightly different current densities to fabricate the APA films. The TEM observations indicate that for the Al films with the same thicknesses, the ordering of nanopore arrangement is better in the APA films with a large current density than that with a small current density. Large current density (or high field) usually leads to highly ordered pore arrangement because of the interacting repulsive force between the alumina cells that is associated with the expansion during oxide formation at the aluminum/oxide interface. This implies that the current fluctuation caused by heat dissipation is also an important factor for formation of ordered pore array. Hence, a low growth temperature will reduce both thermal agitation and fluctuation of the heat

dissipation and make the ordering of nanopore arrangement better.

Under the selected experimental conditions (an applied voltage of dc 20 V, a sulfuric acid concentration of 15 wt.%, an Al film thickness of 0.44 μm, and a growth temperature of 5 °C), the anodizing process of Al film on Si substrate for forming an alumina template with relatively ordered 25 nm nanopores was carried out by controlling the anodizing I–t curve. Although the I–t curve of the aluminum film on Si substrate has been reported in some studies [30,31], our experimental results show new features. A typical I–t curve of the Al/Si system is presented in Fig. 3(a). Corresponding to points A, B, C, and D in the process of anodization, four APA films on Si substrates can be obtained by turning off the current at the corresponding moment. These samples were then treated under open circuit condition in 5 wt.% H_3PO_4 for a long time to detach the APA films from the Si substrates. Therefore, four resultant products A, B, C, and D without the APA films can be obtained. The experimental FTIR transmittance spectra of the four products are illustrated in Fig. 3(b). From curve A, we can infer that the silicon oxide has not yet been formed at point A because no IR vibration band was observed. In curves B, C, and D, an obvious transmittance band appears at 1071 cm^{-1}, which corresponds to the Si–O–Si stretching vibration in stoichiometric SiO_2 [32]. In addition, the 950 cm^{-1} transmittance band related to Si–O–Si bending vibration is also
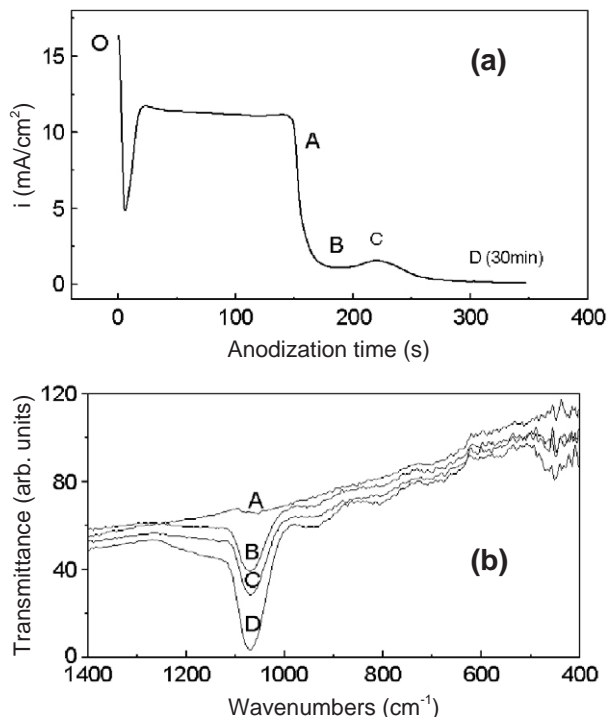

Fig. 3. (a) Current density vs anodizing time during the anodization of the Al/Si system. (b) FTIR transmittance spectra of products A, B, C, and D without the APA films. The anodizing process of the Al/Si system was conducted under a constant voltage of 20 V, a sulfuric acid concentration of 15 wt.%, an Al film thickness of 0.44 μm, and a growth temperature of 5 °C.

noticeable. The intensities of the two bands increase with anodizing time t, indicating that the Si oxide formed during anodization is stoichiometric SiO_2 and its content initially increases with t and finally trends to saturate.

According to the above FTIR results, we can analyze the origin of the $I-t$ curve. The O–A range in Fig. 3(a) is the anodization for the Al film. It undergoes an unstable anodizing process for about 20 s due to a high sulfuric acid concentration. The B–D range is the anodization for the Si substrate. The A–B range is a transformation region. At point B, the anodization on the Al film has run to the interface of the Al/Si system, and will start to thin the alumina barrier layer; in the meantime, it will oxidize the Si substrate to form a Si oxide nanolayer. This layer of Si oxide will undergo a partial potential and thus make the current reduced. Around point C, one can see that the current first reaches a maximum and then drops again. This is because in the B–C range the silicon oxide formed at the Al/Si interface shares most of the applied voltage. This causes an increase of the electric field in the Si oxide layer. Under action of the electric field, ionic conductivity will increase so that oxygenic anions with high energies in the solution can pass through the silicon oxide. Since ionic conductivity increases with the electric field, the current rises. Afterwards, with increasing the anodic time, the silicon oxide layer thickens. When the thickness of the oxide layer increases to a certain extent, the electric field begins to decrease because of the constant applied voltage. Thus, ionic conduction current is reduced again. As a result, there exists a maximal current at point C. To show this kind of the APA structure on Si substrate, a cross-sectional TEM image, taken by monitoring at point D, is presented in Fig. 4(a). The TEM sample was prepared by first cross-sectional cutting the APA film on Si substrate and mechanical grinding to micrometer scale and then by ion beam thinning under small angle of incidence until perforation of the film to obtain an electron transparent area of the sample. One can see that some islands clearly exist at the bottoms of nanopores. To identify their structure, we give a high-resolution TEM image of some islands in the inset. It can be seen that these islands are not voids formed at the interface between alumina film and Si substrate [21,22]. From the FTIR result, we can infer that these islands should be SiO_2. Our energy-dispersive X-ray fluorescence result also confirms this inference. From the TEM image, we may imagine that for an APA film on Si substrate with an ordered nanopore arrangement, the SiO_2 islands formed on the surface of Si substrate will also be arrangement-ordered. To demonstrate this point, we carried out AFM observations of the Si substrate surface. Since the surfaces of products A, B, and C without the APA films have large surface fluctuation, we only present an AFM image of the surface of product D in Fig. 4(b). It can be seen that the mean diameter of the SiO_2 islands is in the range of about 25–30 nm, which is larger than that of the corresponding nanopore sizes. Their distribution is uniform and has a local hexagonal symmetry,
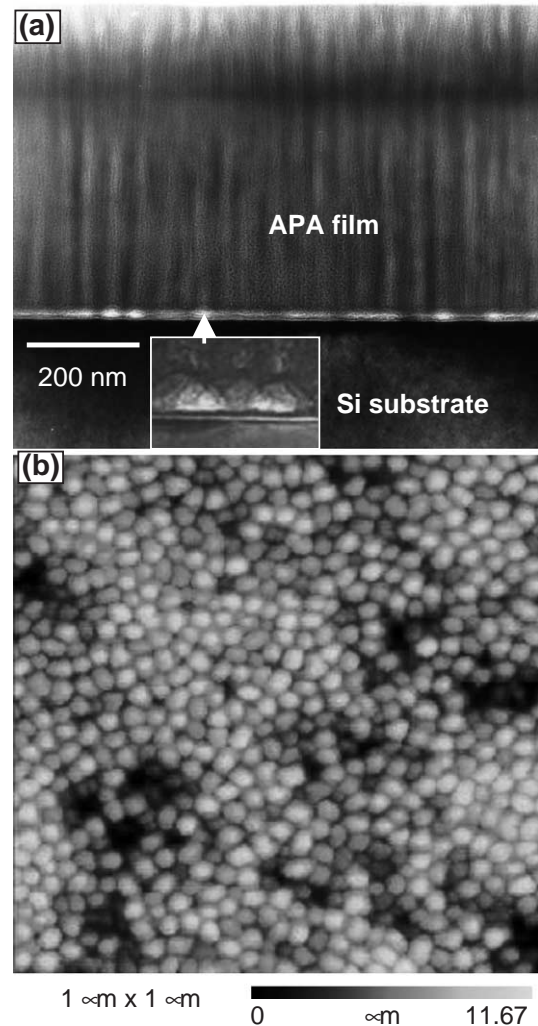

Fig. 4. (a) Cross-sectional TEM image of the APA template on Si substrate fabricated at point D of the $I-t$ curve. The inset shows a high-resolution TEM image of SiO_2 islands. (b) An AFM image of the Si substrate surface from sample D.

as in the case for nanopore distribution in the APA film. However, we can see that the ordering still needs to be improved. This work is currently under way. This kind of SiO_2 quantum dot array can be expected to have practical applications in nano-electronics and nano-optoelectronics.

As an application of the APA template with 25 nm nanopores, we present the fabrication of a Si nanocrystal-embedded APA film on the Si substrate. We first grow an APA film under proper experimental conditions by controlling the $I-t$ curve around point B and then immerse the film in a solution of 5 wt.% H_3PO_4 for open circuit etching of 30 min. This leads to dissolution of the barrier layer at the interface between the APA film and the Si substrate. Finally, we embed Si nanocrystals with sizes less than 20 nm into the nanopores of the APA film through physical deposition and post-processing. Thus we obtain a useful Si nano-crystal-embedded APA film, which can expect to show many new physical phenomena. Spectral measurements indicate that this kind of Si quantum dots is of interesting

light-emitting property and could therefore be used in advanced electronic devices.

4. Conclusion

We have elucidated the anodizing process of Al film on Si substrate for forming an APA template with 25 nm nanopores by analyzing both anodizing $I - t$ curve and infrared transmittance spectroscopy. It is revealed that the ordering of nanopore arrangement is closely related to the thickness of the deposited Al film, the applied voltage, the growth temperature, and the solution concentration. These parameters are explored in our experimental conditions. This kind of APA templates will be suitable for synthesis of some Si-based nanostructures. In addition, a SiO_2 island array is found to exist on the surface of Si substrate under our experimental conditions. The SiO_2 island array can be expected to have applications in nanoelectronics and optoelectronics.

Acknowledgment

References

[1] C.R. Martin, Science 266 (1994) 196.
[2] J.H. Wu, L. Pu, J.P. Zou, Y.F. Mei, J.M. Zhu, X.M. Bao, Chin. Phys. Lett. 17 (2000) 451.
[3] K. Nielsch, F. Müller, A.P. Li, U. Gösele, Adv. Mater. 8 (2000) 582.
[4] C.A. Huber, T.E. Huber, M. Sadoqi, J.A. Lubin, S. Manalis, C.B. Prater, Science 263 (1994) 800.
[5] L. Piraux, S. Dubois, J.L. Duvail, K. Ounadjela, A. Fert, J. Magn. Magn. Mater. 175 (1997) 127.
[6] H. Masuda, K. Fukuda, Science 268 (1995) 1466.
[7] C.B. Murray, D.J. Norris, M.G. Bawendi, J. Am. Chem. Soc. 115 (1993) 8706.
[8] D. Routkevitch, T. Bigioni, M. Moskovits, J.M. Xu, J. Phys. Chem. 100 (1996) 14037.
[9] D.S. Xu, X.S. Shi, G.L. Guo, L.L. Gui, Y.Q. Tang, J. Phys. Chem., B 104 (2000) 5061.
[10] P. Hoyer, Langmuir 12 (1996) 1411.
[11] H. Masuda, T. Yanagishita, K. Yasui, K. Nishio, I. Yagi, T.N. Rao, A. Fujishima, Adv. Mater. 13 (2001) 247.
[12] J. Li, C. Papadopoulos, J.M. Xu, Appl. Phys. Lett. 75 (1999) 367.
[13] T. Iwasaki, T. Motoi, T. Den, Appl. Phys. Lett. 75 (1999) 2044.
[14] J.S. Suh, J.S. Lee, Appl. Phys. Lett. 75 (1999) 2047.
[15] J. Li, C. Papadopoulos, J. Xu, Nature 402 (1999) 254.
[16] C. Papadopoulos, A. Rakitin, J. Li, A.S. Vedeneev, J.M. Xu, Phys. Rev. Lett. 85 (2000) 3476.
[17] M.H. Huang, S. Mao, H. Fieck, H. Yan, Y. Wu, H. Kind, E. Weber, R. Russo, P. Yang, Science 292 (2001) 1897.
[18] K.D. Hirschman, L. Tsybeskov, S.P. Duttagupta, P.M. Fauchet, Nature 384 (1996) 338.
[19] A.P. Li, F. Müller, A. Birner, K. Nielsch, U. Gösele, J. Appl. Phys. 84 (1998) 6023.
[20] J.P. O'Sullivan, G.C. Wood, Proc. R. Soc. Lond., A Contain. Pap. Math. Phys. Character 317 (1997) 511.
[21] S.Z. Chu, K. Wada, S. Inoue, S. Todoroki, Y.K. Takahashi, K. Hono, Chem. Mater. 14 (2002) 4595.
[22] D. Crouse, Y. Lo, A.E. Miller, M. Crouse, Appl. Phys. Lett. 76 (2000) 49.
[23] R.E. Cavicchi, R.H. Silsbee, Phys. Rev. Lett. 52 (1994) 1453.
[24] W.P. Halperin, Rev. Mod. Phys. 58 (1986) 532.
[25] S.Z. Chu, K. Wada, S. Inoue, S. Todoroki, J. Electrochem. Soc. 149 (2002) B321.
[26] Z.J. Sun, H.K. Kim, Appl. Phys. Lett. 81 (2002) 3458.
[27] H. Masuda, K. Yasui, Y. Sakamoto, M. Nakao, T. Tamamura, K. Nishio, Jpn. J. Appl. Phys. 40 (2001) L1267.
[28] H. Masuda, Appl. Phys. Lett. 71 (1997) 2770.
[29] F.Y. Li, L. Zhang, R.M. Metzger, Chem. Mater. 10 (1998) 2470.
[30] H. Asoh, M. Matsuo, M. Yoshihama, S. Ono, Appl. Phys. Lett. 83 (2003) 4408.
[31] S. Ono, M. Saito, M. Ishiguro, H. Asoh, J. Electrochem. Soc. 151 (2004) B473.
[32] P.G. Pai, S.S. Chao, Y. Takagi, J. Vac. Sci. Techol., A Vac. Surf. Films 4 (1996) 689.